Structural diversity of mitochondria in the neuromuscular system across development

J. Alexander Bae[1, †, *], Myung-kyu Choi[2, †], Soungyub Ahn[2, †], Gwanho Ko[2], Daniel T. Choe[2], Hyunsoo Yim[2], Ken C. Nguyen[3], David H. Hall[3,6], Jinseop S. Kim[4,5,6], Junho Lee[2,6,*]

[1] Research Institute of Basic Sciences, Seoul National University, Seoul, Republic of Korea
[2] Department of Biological Sciences, Seoul National University, Seoul, Republic of Korea
[3] Dominick P. Purpura Department of Neuroscience, Albert Einstein College of Medicine, Bronx, NY, USA
[4] Department of Structure and Function of Neural Networks, Korea Brain Research Institute, Daegu, Republic of Korea
[5] Department of Biological Sciences, Sungkyunkwan University, Suwon, Republic of Korea
[6] Senior authors
[†] These authors contributed equally.

[*]Correspondence: jabae@snu.ac.kr, elegans@snu.ac.kr

Abstract

As an animal matures, its neural circuit undergoes alterations, leading to changes in both neuronal morphology and the connectivity between neurons. However, less is known about the mitochondrial structure changes across development to facilitate these changes, while mitochondria are highly dynamic organelles related to neuronal development. Here, we attempt to answer this question with a model organism *C. elegans* using 3D electron microscopy (EM). We developed semi-automated methods for reconstructing mitochondria in *C. elegans* EM images using deep learning. Consequently, we collected mitochondria reconstructions from normal reproductive stages and dauer, enabling comparative study on mitochondrial morphology and spatial organization within the neuromuscular system across different stages. We have identified that the mitochondria structural properties in neurons are correlated with synaptic properties. Neuronal compartments have distinct roles, leading axonal mitochondria to differ morphologically from dendritic mitochondria. We tested this by analyzing behavior in animals with a mutation in *drp-1*, required for proper mitochondrial fission, confirming that compartment-specific mitochondrial morphology is vital for effective functioning of synapses. Given that these functions are essential throughout development, the structural properties of mitochondria are preserved across development. We report that dauer inter- and motor neurons, predominantly cholinergic and glutamatergic, show distinctive mitochondrial structure and increased mitochondria density. In addition, mitochondria in dauer body wall muscles exhibit distinctive reticulum-like structure. We propose that the stage-specific mitochondrial structure observed in *C. elegans* dauer may constitute an adaptive mechanism to support stage-specific behavioral and physiological characteristics.

Introduction

The neural circuit undergoes continuous changes throughout development in various brain regions, adapting for more complex computations and to perform more resilient behavior (*Neural Circuit Development and Function in the Healthy and Diseased Brain: Comprehensive Developmental Neuroscience* 2013; Tau and Peterson 2010). This functional adaptation across development is accompanied by the structural alterations, resulting in changes to both neuronal morphology and connectivity between neurons (Grueber et al. 2005; Kroon et al. 2019; Khalil, Farhat, and Dłotko 2021; Kolk and Rakic 2022; Witvliet et al. 2021; Mulcahy et al. 2022). To induce changes in neuronal morphology and connectivity, numerous intracellular organelles participate in the process, with mitochondria playing a central role through trafficking and reshaping (Harris, Jolivet, and Attwell 2012; Verstreken et al. 2005; Kimura and Murakami 2014; Sheng and Cai 2012; Courchet et al. 2013). However, less is known about how mitochondrial structure evolves throughout development to support diverse neural circuits and cellular processes.

3D electron microscopy (EM) provides a distinctive advantage in studying structural properties of mitochondria due to its superior resolution. It allows us to study not only the detailed morphology of individual mitochondrion but also the overall organization of all mitochondria in the volume. Besides, it enables us to relate the mitochondrial structural properties with other cellular features such as neurite morphology and synapses since it contains various structural information.

Previously, a number of studies investigated mitochondrial structure using 3D EM in mammalian neurons (Kasthuri et al. 2015; Smith et al. 2016; Bloss et al. 2018; Calì et al. 2018; Turner et al. 2022). However, as mammalian neural circuits are quite large, most studies were limited to a small number of neurons or to selected regions of the brain. In invertebrates, a comprehensive study on mitochondrial structure in *Drosophila* has been reported recently; however, this study did not include analysis of muscle cell mitochondria (Rivlin et al. 2024). In order to gain deeper insights into the connection between mitochondrial structure and neural circuit function, it is essential to investigate mitochondrial structure within an entire system from sensory neurons to muscle cells as there could be regional differences in the neuromuscular system (White et al. 1986).

Besides, most EM studies on mitochondria are limited to single time point (Kasthuri et al. 2015; Smith et al. 2016; Bloss et al. 2018; Turner et al. 2022; Rivlin et al. 2024). When multiple time points are examined, the studies compare only a few broadly defined intervals like young adult vs. aged (Calì et al. 2018). However, these time points are rather ill-defined, making it difficult to identify stereotypic cellular or circuit functions at each interval. In contrast, *C. elegans* developmental stages are clearly distinguishable, and numerous studies have reported findings on stage-specific cellular physiology and behavior in an alternative developmental stage (Cassada and Russell 1975; Golden and Riddle 1984a, 1984b; Gaglia and Kenyon 2009; Hallem et al. 2011; Wolkow and Hall 2016; H. Lee et al. 2011).

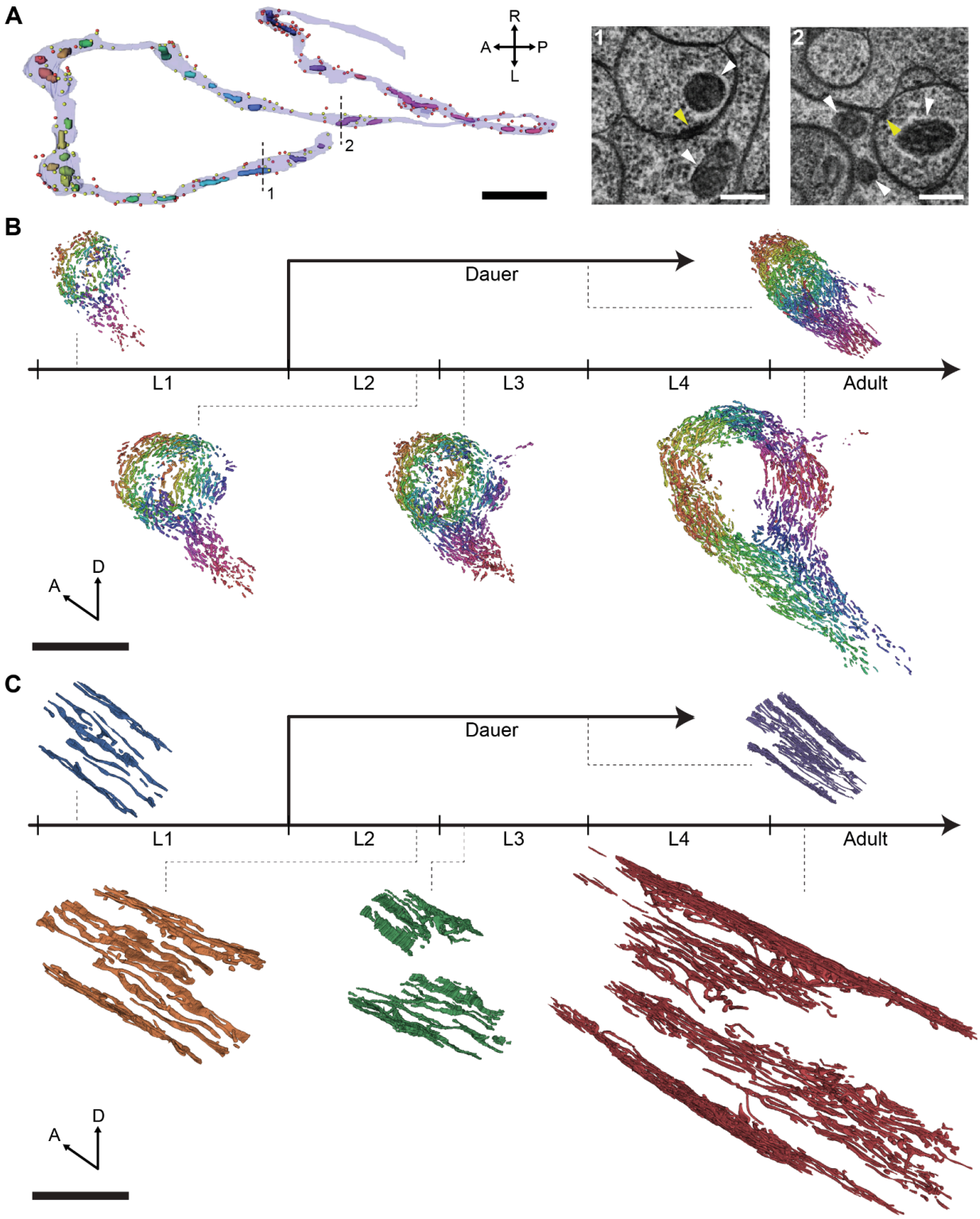

Figure 1. Dense reconstructions of mitochondria of *C. elegans* across development. (A) Mitochondria reconstructions in a sample neuron, RIAR, in the dauer stage with presynaptic sites (i.e., active zones; yellow circles) and postsynaptic sites (red circles) labeled (left). Parts of thin sections at the locations indicated by dashed lines (right) including mitochondria (white arrows) and active zones (yellow

arrows). (B and C) Dense neuronal mitochondria (B) and body wall muscle mitochondria (C) reconstructions in different developmental stages: L1, L2, L3, adult, and dauer.
(A) Scale bars: 2 μm (black), 200 nm (white). (B and C) Scale bar: 10 μm. (A and B) Different mitochondria are denoted by colors. (C) Colors of mitochondria indicate their stage.

Here we use 3D EM and *C. elegans* as a model organism to answer the above questions as it becomes feasible to conduct a comprehensive analysis of mitochondrial structure within an entire system across development. We have densely reconstructed mitochondria from 3D EM images in the *C. elegans* body near the nerve ring for various developmental stages from L1 to adult, and dauer stage (Figure 1; Witvliet et al. 2021; Yim et al. 2024). Our EM reconstructions provide us with opportunities to study detailed mitochondria structure in both neuronal and muscle cells across multiple developmental stages from the initial L1 stage after the egg hatch to adult, and also the alternative long-lived stage, the dauer. Consequently, we found that there exists fundamental principles in mitochondrial structure that are conserved across development. In addition, we have tested that this specific structure is necessary to operate the neural circuit resulting in the intended behavior. Lastly, we observed that mitochondria in the dauer stage exhibit distinct morphology, providing insights into their role during the energy-conserving phase.

Results

Comprehensive mitochondria reconstructions in different developmental stages

Mitochondria have distinctive visual features in EM (Figure 1A) so it is feasible to visually identify mitochondria in EM. Consequently, we have trained a convolutional neural network (CNN) to automatically detect mitochondria in each image section (Figure S1A, STAR Methods). Then, we have reconstructed mitochondria in 3D by combining predictions from adjacent sections (Figure S1A, STAR Methods).

We have densely reconstructed mitochondria in different developmental stages of *C. elegans*: L1, L2, L3, adult, and dauer (Figures 1B and 1C). For normal reproductive stages, we have used publicly available EM image volumes which have been published recently (Witvliet et al. 2021). For dauer, we imaged the *C. elegans* dauer with length of ~18 μm using serial-section EM (Yim et al. 2024). We have reconstructed all the mitochondria, both in neuronal and non-neuronal cells like body wall muscles (BWMs), included in the EM volume (Figures 1B and 1C).

In the neurites of neurons, mitochondria exist in pill-shaped pieces and they rarely have branching (Figure 1B). The total number of mitochondria in neurons had a linearly increasing trend from L1 to adulthood, approximately a five-fold increase (Figure S1B; L1: n=461, L2: n=816; L3: n=1043, Adult: n=2121). This is similar to the increase in neurite length and body length from L1 to adulthood (Witvliet et al. 2021). In the dauer stage, neurons contained about 30% more mitochondria than neurons in L3 (n=1301), which is a similar stage in terms of developmental cycle (Figure S1B).

The size of individual mitochondrion increased from L1 to L2, then the size of mitochondrion saturated to a similar level from L2 to adult (Figure S1C). While the number of mitochondria in

the dauer was slightly larger than that of L3 (Figure S1B), the volume of mitochondrion was substantially smaller in the dauer, while the length of mitochondrion was comparable (Figure S1C). As more, larger, and longer mitochondria exist in adult neurons, mitochondria in the nerve ring showed eight-fold increase in total volume (Figure S1D). The dauer stage showed similar values with stages L2 and L3 (Figure S1D).

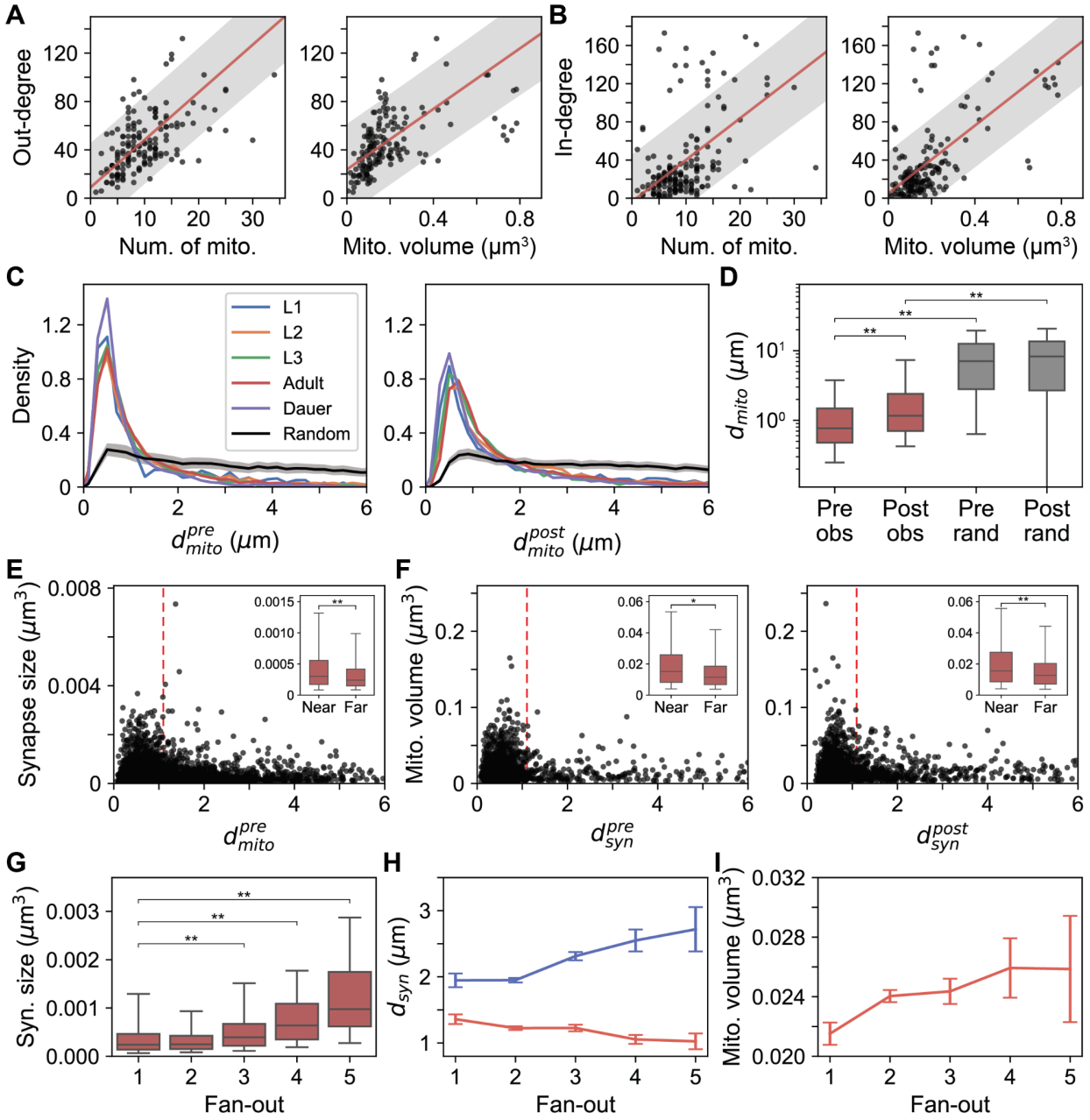

Figure 2. Mitochondria structure is related to synaptic connections. (A) Out-degree is positively correlated with number of mitochondria in neuron (left: r=0.65, p<10^{-19}; Pearson correlation) and sum of the mitochondria volume in neuron (right: r=0.62, p<10^{-17}; Pearson correlation). RIAs are not shown for visualization purposes as they have outlying out-degree (see Figure S2). (B) Same with (A) for in-degree (left: r=0.56, p<10^{-15}; right: r=0.68, p<10^{-24}; Pearson correlation). (C) Distance to nearest mitochondria from presynaptic (left) and postsynaptic (right) sites in different developmental stages (color lines) and

distance to randomly assigned mitochondria (black line). Area under the curve is normalized to be equal to 1. (D) Distance to postsynaptic sites is greater than distance to presynaptic sites ($p \approx 0$) and distance to randomly assigned mitochondria is significantly larger than distance to nearest mitochondria ($p \approx 0$). (E) Active zones near (below red dashed) mitochondria are larger (inset) than those farther away ($p<10^{-11}$). (F) Mitochondria near (below red dashed) synapses are larger (inset) than those farther away for both pre- (left; $p<10^{-4}$) and postsynaptic sites (right; $p<10^{-5}$). (G) Active zone sizes tend to be larger for synapses with larger fan-out (from left; $p<10^{-15}$, $p<10^{-19}$, $p<10^{-12}$). (H) Mitochondria are located closer to presynaptic sites (red) and farther away from postsynaptic sites (blue) for synapses with larger fan-out. (G) Mitochondria near presynaptic sites are larger for synapses with larger fan-out.
(A and B) Line: linear fit, shade: 80% prediction interval. (C) Black line: mean, black shade: 95% confidence interval. (D-G) Center line: median, box: interquartile range, whiskers: 5th and 95th percentile. *$p<10^{-4}$, **$p<10^{-5}$; Wilcoxon rank-sum test. (A-I) Adult data are shown as representative.

In the BWMs, mitochondria exist in elongated form spanning over the muscles, which is expected as the mitochondria need to provide energy in every location along the body. As the worm develops from L1 to adult, the mitochondria form more branches leading to more complex shape with aligned strands, similar to the previous report (Figure 1C; Han et al. 2012; Schultz et al. 2017). The BWM mitochondria in dauer has more branching as in adults but are composed of sparser strands which we will elaborate in the later section (Figure 1C).

Mitochondria structure is related to synaptic connections

Mitochondria are known to be closely associated with synaptic connections. Since we are provided with both the morphology and spatial locations of synapses and mitochondria, it is possible to investigate the relation between them. As a result, we found out-degree, the number of outgoing synapses, is correlated with the number of mitochondria and the total amount of mitochondria in a neuron in all developmental stages (Figures 2A and S2A). Moreover, the amount of mitochondria is also correlated with in-degree, the number of incoming synapses. (Figures 2B and S2B). These results suggest that neurons with more mitochondria tend to form more synaptic connections.

Nevertheless, the correlation between mitochondrial morphology and out-degree does not explain that mitochondria and synapses are spatially correlated, as mitochondria can be concentrated at certain locations in neurites regardless of synapse locations. Therefore, we measured the distance from each active zone (d_{mito}^{pre}) and each postsynaptic site (d_{mito}^{post}) to the nearest mitochondria. Looking at the distribution of these distances, we were able to observe a peak within 1 μm in every developmental stage (Figure 2C). Considering the diameter of a bouton in the neurite is approximately in the range of 1 to 2 μm, this means there are mitochondria located at the same bouton where there are outgoing or incoming synapses. Consistent with previous results in *Drosophila*, we found that distances to postsynaptic sites are significantly larger than distances to active zones (Figures 2D and S2C; Rivlin et al. 2024; Riboul et al. 2023). To test this result did not occur by chance, we have assigned a random mitochondria within a neuron for every active zone (STAR Methods) and measured the distance to the nearest mitochondria. We were able to see that the distribution of distances in the randomized configurations were relatively more uniform and the distances in our data were

significantly smaller in the observed configuration for both pre- and postsynaptic sites (Figures 2C and 2D; $p \approx 0$, two-sided t-test).

Mitochondria support synaptic transmission by regulating neurotransmitter release by several mechanisms like calcium buffering. Therefore, mitochondrial proximity to synapses could be important and we hypothesized mitochondria would be closely located to support larger synapses (i.e. larger active zones). Indeed, we found that large synapses tend to have the nearest mitochondria closer than smaller synapses (Figures 2E and S3A). Most of the synapses, over 95%, had similar synapse size, less than 0.001 μm^3 but there were large synapses which have a diverse range of sizes (Figure 2E). Synapses that have mitochondria nearby (see STAR Methods) were significantly larger than synapses with mitochondria farther away (Figure 2E). This result is consistent with study in mammalian neurons (Smith et al. 2016), providing additional evidence for the relationship between mitochondrial proximity and synapse efficacy. Vice versa, we measured the distance to pre- (d_{syn}^{pre}) and postsynaptic (d_{syn}^{post}) from the nearest mitochondria and observed mitochondria located closer to synapses were larger, indicating larger mitochondria are needed to operate larger synapses (Figures 2F, S3B, and S3C).

C. elegans is a polyadic animal, meaning a single active zone can send neurotransmitters to multiple partners. From above results, we hypothesized that active zones with higher fan-out, number of postsynaptic partners, would have larger mitochondria nearby as active zones with larger fanout have larger synapses (Figures 2G and S4A). As expected, the nearest mitochondria were larger and closer to the synapses as fan-out increased (Figures 2H, 2I, S4B, and S4C). On the contrary, nearest mitochondria were farther away at the postsynaptic sites when they shared input with more cells (Figures 2H and S4B). All the relations are consistent among different developmental stages (Figures S2-S4).

Axonal mitochondria are shorter than dendritic mitochondria

Mitochondria structures differ in different compartments (e.g. axon, dendrite, and soma) in mammalian neurons (D. T. W. Chang, Honick, and Reynolds 2006; Lewis et al. 2018b; Turner et al. 2022) as each compartment serves a different function. In *C. elegans* neurons, roles of different compartments are merged as the same neurite can both send and receive signals. However, there are exceptions in symmetric motor neurons. For example, it is known that SMDD and SMDV have outgoing synapses only at boutons in dorsal and ventral regions of arbor (Figures 3A-3C and S5A-S5D) respectively, which leads to compartmentalized activity in RIA (Hendricks et al. 2012). Unlike outgoing synapses, the incoming synapses exist at both boutons (Figures 3A-3C). Other classes of motor neurons, RMDD and RMDV, also show compartmentalized synapse distribution along with SMBD, RMDR and RMDL (Figures 3E, 3F, and S6).

Due to compartmentalized synapse distribution, it is feasible to isolate the neurite region with only incoming synapses, like dendrites, and study whether there is any difference in mitochondria structures. Here, we will define mitochondria in this region with only incoming synapses as “dendritic” and the ones in the other boutons as “axonal” for convenience even

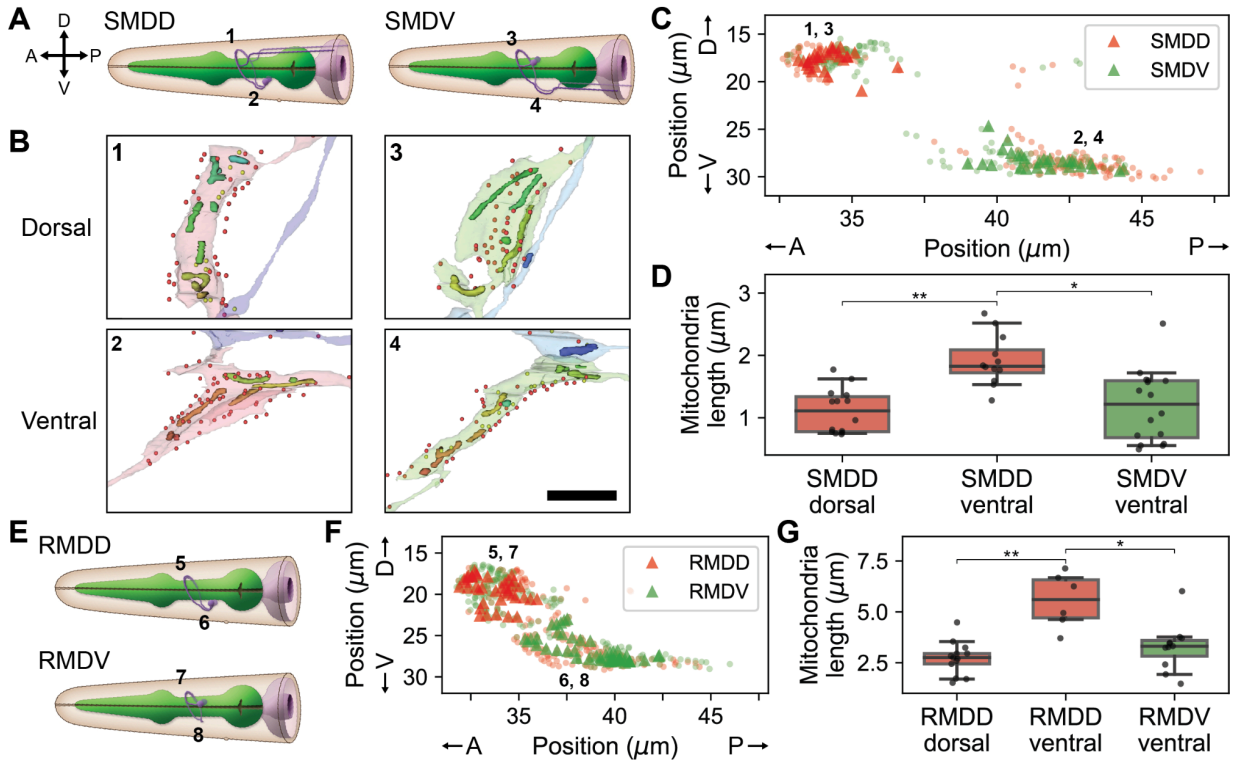

Figure 3. Axonal mitochondria are shorter. (A) Diagram of SMDD (left) and SMDV (right) neurons. (B) Reconstructed mitochondria in adult SMDD (left) and SMDV dorsal (top) and ventral (bottom) boutons. Number indicates locations marked in (A). Presynaptic (yellow) and postsynaptic (red) sites are marked with dots. (C) Distribution of outgoing (triangle) and incoming (circle) synapses of SMDD (red) and SMDV (green). Numbers are locations of numbered boxes in (B). (D) Mitochondria are longer in the ventral bouton of SMDD, where it only receives inputs (left, p=0.00011). Within the ventral boutons, mitochondria are longer in SMDD (right, p=0.00116). (E) Diagram of RMDD (top) and RMDV (bottom) neurons. (F) Same with (C) for RMDD (red) and RMDV (green). (G) Mitochondria are longer in the ventral bouton of RMDD, where it only receives inputs (left, p=0.00086). Within the ventral boutons, mitochondria are longer in RMDD (right, p=0.00356).
(A and E) Diagrams are adopted from WormAtlas (Altun, Z.F. and Hall, D.H. 2024). A: anterior, P: posterior, D: dorsal, V: ventral. (B) Scale bar: 2 μm. (D and G) Center line: median, box: interquartile range, whiskers: 5th and 95th percentile. *p<0.01, **p<0.001; Wilcoxon rank-sum test.

though the boutons have mixed pre- and postsynaptic sites. We discovered that dendritic mitochondria are longer compared to axonal mitochondria in SMD neurons (Figures 3B and S5A-S5D). We have verified this by comparing mitochondria in SMDD dorsal (axonal) and SMDD ventral (dendritic) boutons (Figure 3D). As this result could be due to the difference in the bouton size, when we compared the ventral boutons of SMDD and SMDV, the mitochondria in SMDV ventral (axonal) boutons were smaller than mitochondria in SMDD ventral (dendritic) boutons (Figure 3D). Similar results have been tested with RMD neurons (Figure 3G). This result is consistent with previous findings that dendritic mitochondria tend to be larger and longer (D. T. W. Chang, Honick, and Reynolds 2006; Lewis et al. 2018b; Turner et al. 2022). This structural property is a fundamental principle that can be found in all developmental stages (Figure S5).

Mitochondrial morphology is adapted to accommodate neural circuit function

Above, we have seen that axonal mitochondria have shorter morphology and mitochondria are spatially related to synapses. Therefore, we questioned whether the particular mitochondrial morphology and localization is necessary for proper synaptic transmission, thereby important for intended behavioral output. SMD neurons have been known to be involved in omega turns or sharp directional changes as they activate head and neck muscles (White et al. 1986; Gray, Hill, and Bargmann 2005). Assuming mitochondrial morphology is adapted to support synaptic transmission, we hypothesized disruption of mitochondria structure in SMD neurons would interrupt innervation of body wall muscles, inhibiting the turning behavior.

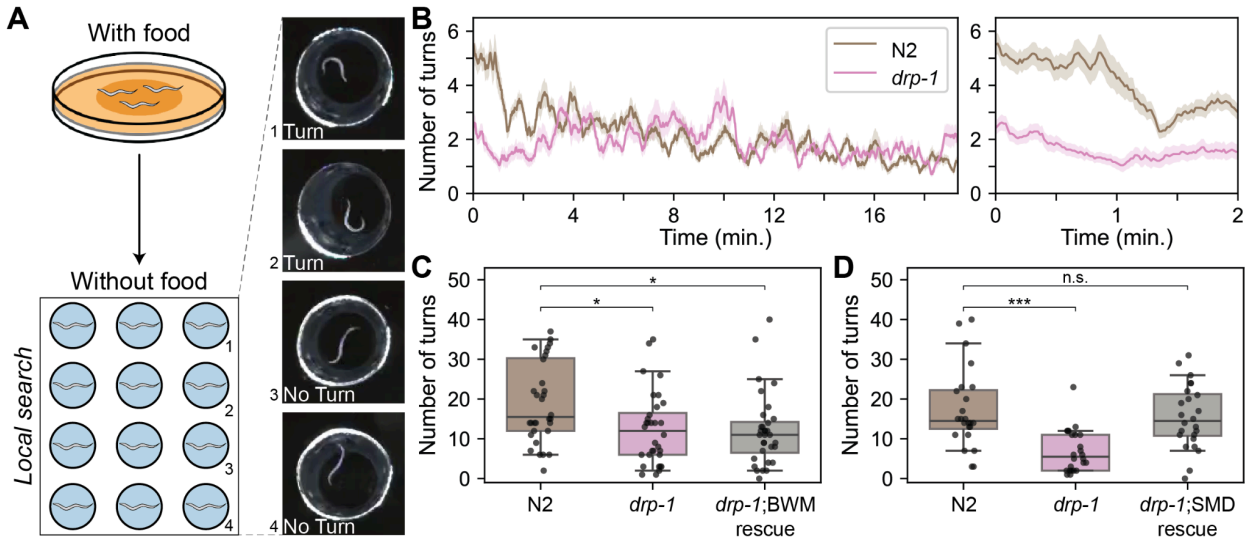

Figure 4. Mitochondrial morphology is adapted to accommodate neural circuit function. (A) Behavior experiment setup. Worms were transferred from the environment with food to the environment without food, then the number of turns were counted. (B) Number of turns over time for 20-minute recording (left) and for first 2-minute recording (right). (C) Total number of turns in the first 2 minutes for N2 wild-type, *drp-1* mutants, and BWM-specific rescue model. *drp-1* mutants exhibit significantly lower number of turns compared to the wild-type and impaired behavior in *drp-1* mutants are not recovered in the BWM-specific rescue model. (D) Same with (C) for SMD neurons and the behavior is recovered in the SMD-specific rescue model.
(C and D) Center line: median, box: interquartile range, whiskers: 5th and 95th percentile. *p<0.01, **p<0.001, ***p<0.0001; Wilcoxon rank-sum test.

In this study, we observed a kind of exploratory behavior, local search, to investigate how mitochondrial structure affects the behavior (Figure 4A; Gray, Hill, and Bargmann 2005). When the animals are removed from food, they make sharp turns to search for food, mediated by SMD neurons, similar to biased random walk (Pierce-Shimomura, Morse, and Lockery 1999; Gray, Hill, and Bargmann 2005). As it has been previously reported, animals showed high turning rate due to local search behavior immediately after they have been transferred to an environment without food (Figure 4B). Then the turning rate saturated to the base rate where they stopped showing local search behavior (Figure 4B). According to our hypothesis, we expected this local search behavior would be impaired when the mitochondrial structure is disrupted.

To test this idea, we checked the local search behavior in the mutants important for the mitochondrial morphology *drp-1*, a mitochondria fission factor. In fact, *drp-1* mutants, where mitochondria fission is interrupted, showed a defect in increased turning rate during local search behavior (Figure 4B). This result suggests that mitochondrial morphology and localization regulated by the mitochondria fission factor is important for proper synaptic function in SMD neurons.

To quantitatively compare the local search behavior, we counted the total number of turns within the first 2 minutes after the worms were transferred, where an increased turning rate was observed in wild-type animals (Figure 4B). The total number of turns were significantly lower in *drp-1* mutants compared to the wild-type as expected (Figures 4C and 4D). However, *drp-1* mutants have broken mitochondria structure in various cells. We first tested whether this deficit in behavior is caused by the disruption of mitochondrial morphology in BWMs as they are the cells that execute the behavior. However, the total number of turns in BWM-specific rescue of *drp-1* mutants were not significantly different from that of *drp-1* mutants (Figure 4C).

With body wall muscles excluded from the candidates, we then moved onto our original hypothesis, that this behavior deficit is due to the dysfunction in SMD neurons, which fails to innervate BWMs. We created SMD-specific rescue of *drp-1* mutants and were able to see the local search behavior recovered to the normal level (Figure 4D). These results imply mitochondrial morphology is adapted to accommodate proper synaptic transmission in neurons to maintain effective functioning of the neural circuit.

Dauer neuronal mitochondria exhibit distinctive structure

Beyond the fundamental structural properties of mitochondria conserved across development, are there any differences? As we have densely reconstructed mitochondria in diverse developmental stages, it enables us to conduct stage-wise quantitative comparison of mitochondria structure. As mitochondrial structure is related to synapses (Figure 2), investigating mitochondrial morphology in the neurons of different stages could provide insights in understanding the differences in neural circuits.

Using dense reconstructions of mitochondria and cells, it allows us to quantitatively measure various mitochondrial morphological features in any given cell. We have computed mitochondria volume, surface area, volume fraction, length, and mitochondria complexity index (MCI). We initially explored an overview of mitochondrial features by projecting all mitochondrial features onto principal components. As a result, we observed that several dauer neurons distinctly separated from the majority (Figure 5A).

Neurons in *C. elegans* are classified into three types - sensory, inter-, and motor neurons - depending on their functions. Variability in function can be encoded in the structure as the cell shapes of different types differ and mitochondria structure can also differ accordingly. In most of the stages, no significant difference in the distribution of mitochondria volume was observed between different cell types, even though there were some interneurons and motor neurons that possessed large amounts of mitochondria (Figure 5B). On the other hand, motor neurons in dauer had more mitochondria in volume on average compared to interneurons and sensory

neurons (Figure 5B). Moreover, interneurons in dauer had significantly more mitochondria than sensory neurons (Figure 5B).

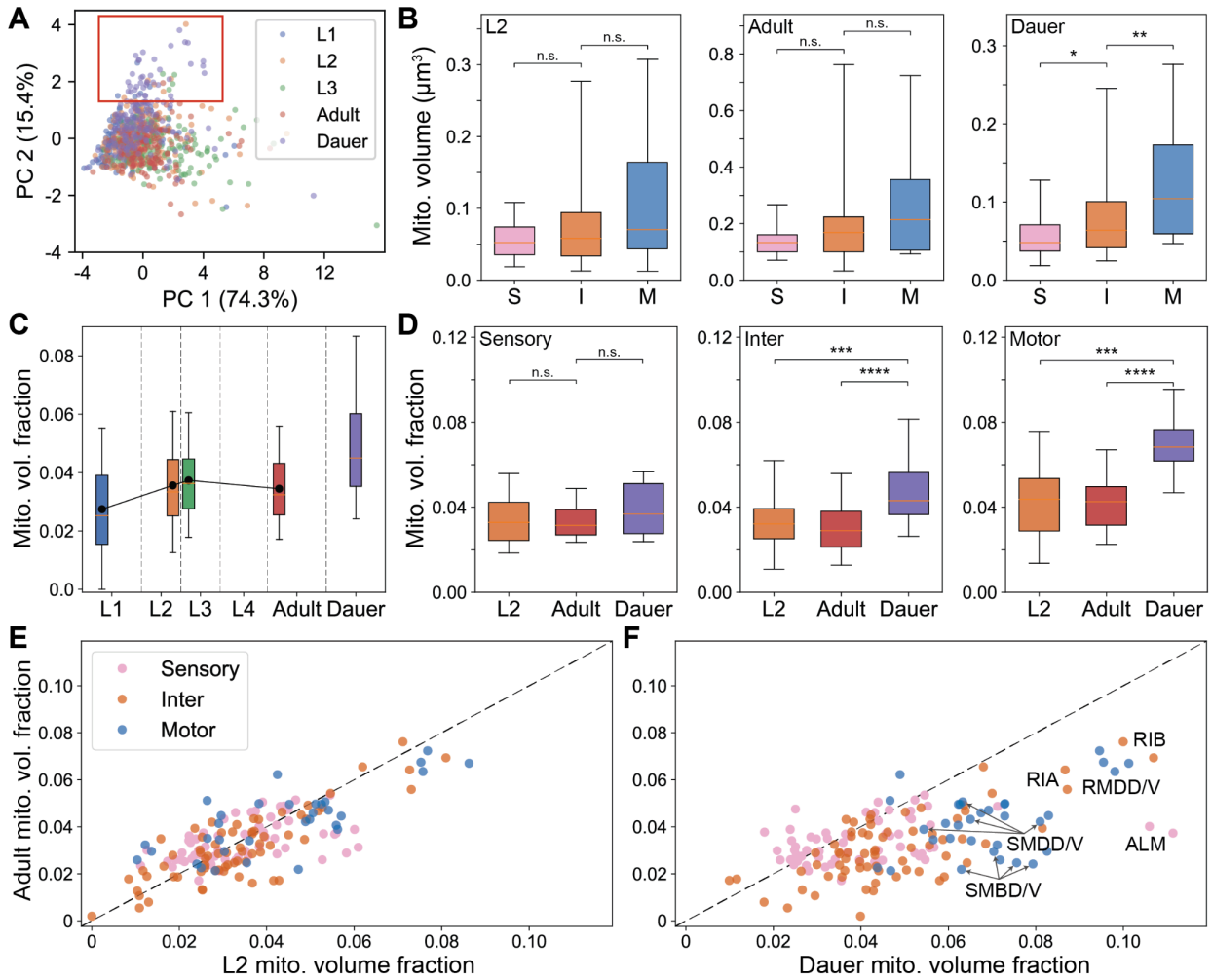

Figure 5. Dauer inter- and motor neurons show distinctive mitochondrial features. (A) Principal component embeddings of neuronal mitochondria features show group of dauer neurons clustered outside (red box). (B) Distribution of mitochondria volume in neurons per type for L2 (left), adult (middle), and dauer (right). (C) Distribution of mitochondria proportion across development. (D) Distribution of mitochondria proportion per different developmental stages for sensory (left), inter- (middle), and motor (right) neurons. (E and F) Comparison between mitochondria proportion or L2 and adult (E) and mitochondria proportion of dauer and adult (F). Dauer shows higher mitochondria proportion relative to other developmental stages.
(C) Black: mean. (B-D) Orange line: median, box: interquartile range, whiskers: 5th and 95th percentile. (B and D) *p<0.05, **p<0.01, ***p<10^{-6}, ****p<10^{-7}; Wilcoxon rank-sum test.

Still, we lack evidence to draw conclusions regarding stage-wise comparisons because size of neurons differ between stages and it is obvious that larger cells are likely to have more mitochondria (Figures S1C-S1E). In order to compensate for this caveat, we introduced a new measure, mitochondria proportion, where we divide the total mitochondria volume in a neuron by the neuron arbor volume. Unlike the mitochondria volume, mitochondria proportion was

constant in normal reproductive stages, from L1 to adult stages except for the dauer stage, where the mitochondria proportion was exceptionally high (Figure 5C). When we analyzed per cell types, the mitochondria proportion of neurons in dauer were significantly greater in interneurons and motor neurons while the difference is negligible in sensory neurons (Figure 5D). As the amount of mitochondria is correlated with number of connections, this result could imply increased role of motor neurons in neural circuits of dauer compared to normal reproductive stages, which is consistent with recent findings in *C. elegans* dauer connectome (Yim et al. 2024).

To verify that this difference of mitochondria proportion is true for the same neuron in different stages, we looked at the mitochondria proportion of individual neurons (Figures 5E and 5F). Mitochondria proportion in neurons of L2 and adult were similar (Figure 5E) while mitochondria proportion of neurons in dauer were larger for many neurons (Figure 5F). As we saw from the distributions, many interneurons and motor neurons tend to have higher mitochondria proportion (Figure 5F), especially neurons involved in head and neck movement (Gray, Hill, and Bargmann 2005).

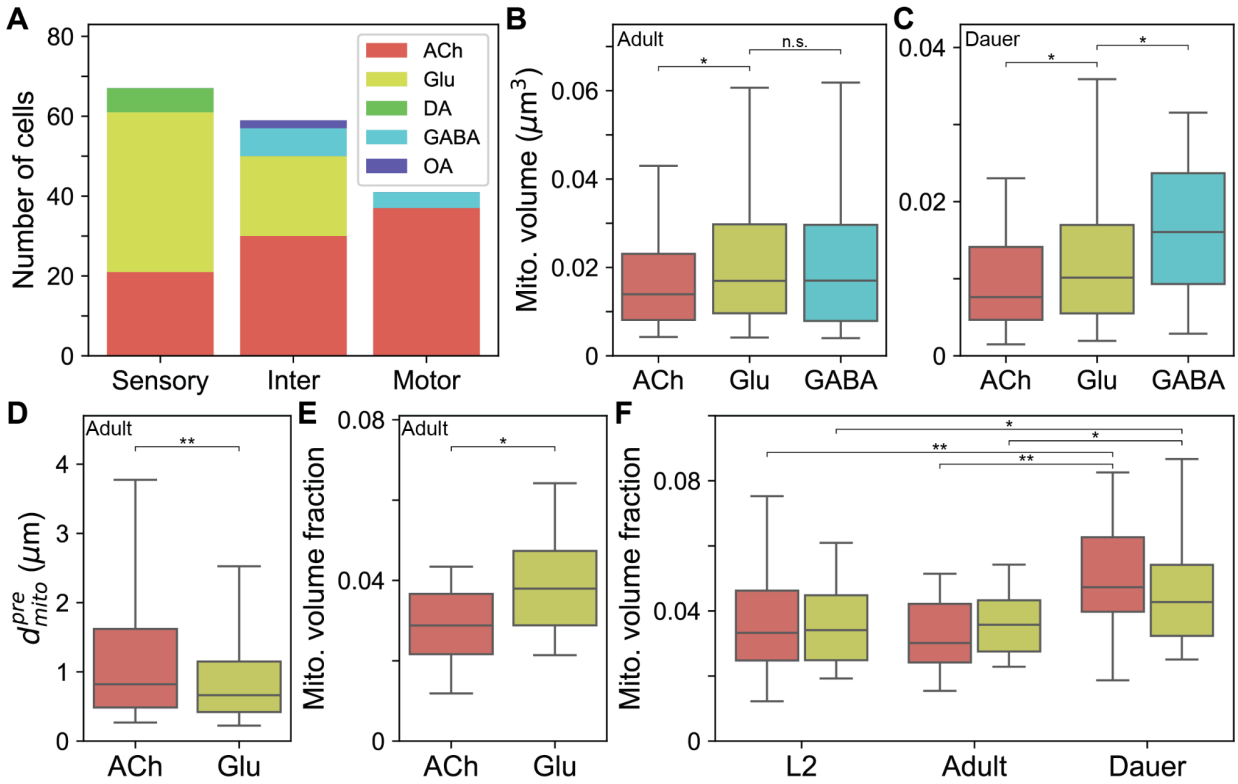

Figure 6. Dauer cholinergic and glutamatergic neurons show distinctive mitochondrial features. (A) Proportion of neuron types by neurotransmitter classification for each cell type. (B) Glutamatergic interneurons have larger mitochondria than cholinergic interneurons (p=0.001). (C) Same with (B) but GABAergic interneurons have larger mitochondria than glutamatergic interneurons in dauer (p=0.002; p=0.007). (D) Glutamatergic interneurons have mitochondria closer to active zones than cholinergic interneurons ($p<10^{-5}$). (E) Glutamatergic interneurons have higher mitochondria volume fraction than cholinergic interneurons (p=0.007). (F) Dauer cholinergic ($p<10^{-6}$; $p<10^{-8}$) and glutamatergic neurons (p=0.003; p=0.003) have higher mitochondria volume fraction.

(B-F) Center line: median, box: interquartile range, whiskers: 5th and 95th percentile. *$p<0.01$, **$p<10^{-5}$ Wilcoxon rank-sum test.

Neurons can be categorized by their functions, but they can also be classified based on the neurotransmitters they release (Hobert, Glenwinkel, and White 2016). Due to mitochondria being responsible for neurotransmitter release, it is plausible that mitochondria structure can depend on neurotransmitter identities.

In *C. elegans*, most neurons release acetylcholine (ACh) and glutamate (Glu), with sensory and interneurons primarily consisting of cholinergic and glutamatergic types (Figure 6A). Additionally, a few sensory neurons release dopamine, while several interneurons release GABA (Figure 6A). For this study, we restricted our analysis on the three predominant neurotransmitters - ACh, Glu, and GABA - since neurons releasing other neurotransmitters are too few to draw reliable conclusions.

We focused our analysis on interneurons because these neurons primarily connect with other neurons rather than non-neuronal cells, emphasizing their central role in neural communication. Among interneurons, we found that mitochondria in glutamatergic and GABAergic neurons have larger mitochondria than those in cholinergic neurons in normal reproductive stages (Figure 6B). Alternatively, GABAergic neurons possess even larger mitochondria than glutamatergic neurons (Figure 6C). Furthermore, we also observed that glutamatergic neurons have mitochondria more closely located to active zones (Figure 6D) and have higher mitochondria volume fraction (Figure 6E). These results are consistent with previous findings in *Drosophila* whole brain, indicating it could be a shared characteristic among invertebrates (Rivlin et al. 2024).

From above results, it can be inferred that more prominent mitochondria are necessary in glutamatergic and GABAergic neurons (Figures 6B-6E). Considering GABA is inhibitory neurotransmitter and glutamate can act as inhibitory neurotransmitter in some neurons like AIB and RIM, this result could be suggesting inhibitory interneurons require more energy per cell compared to other excitatory neurons (Kann 2016; Rivlin et al. 2024).

When comparing different stages, we noticed that both cholinergic and glutamatergic neurons in dauer, regardless of the types, show higher mitochondria volume fraction than normal reproductive stage (Figure 6F). Acetylcholine and glutamate are known to play crucial roles during the dauer stage such as modulating behavioral responses specific to the dauer stage. The mitochondrial structure could have been adapted to accommodate this stage-specific phenomenon.

Dauer body wall muscle mitochondria exhibit distinctive structure

We have not only reconstructed neuronal mitochondria but also reconstructed those in BWMs, allowing us to make structural comparisons of BWM mitochondria across development. The BWMs included in the data are head and neck muscles as our study has been centered around the vicinity of the nerve ring.

Interestingly, the morphology of mitochondria in head and neck muscles undergoes substantial changes throughout the developmental stages (Figure 7A). In L1, muscle cells contain a solitary

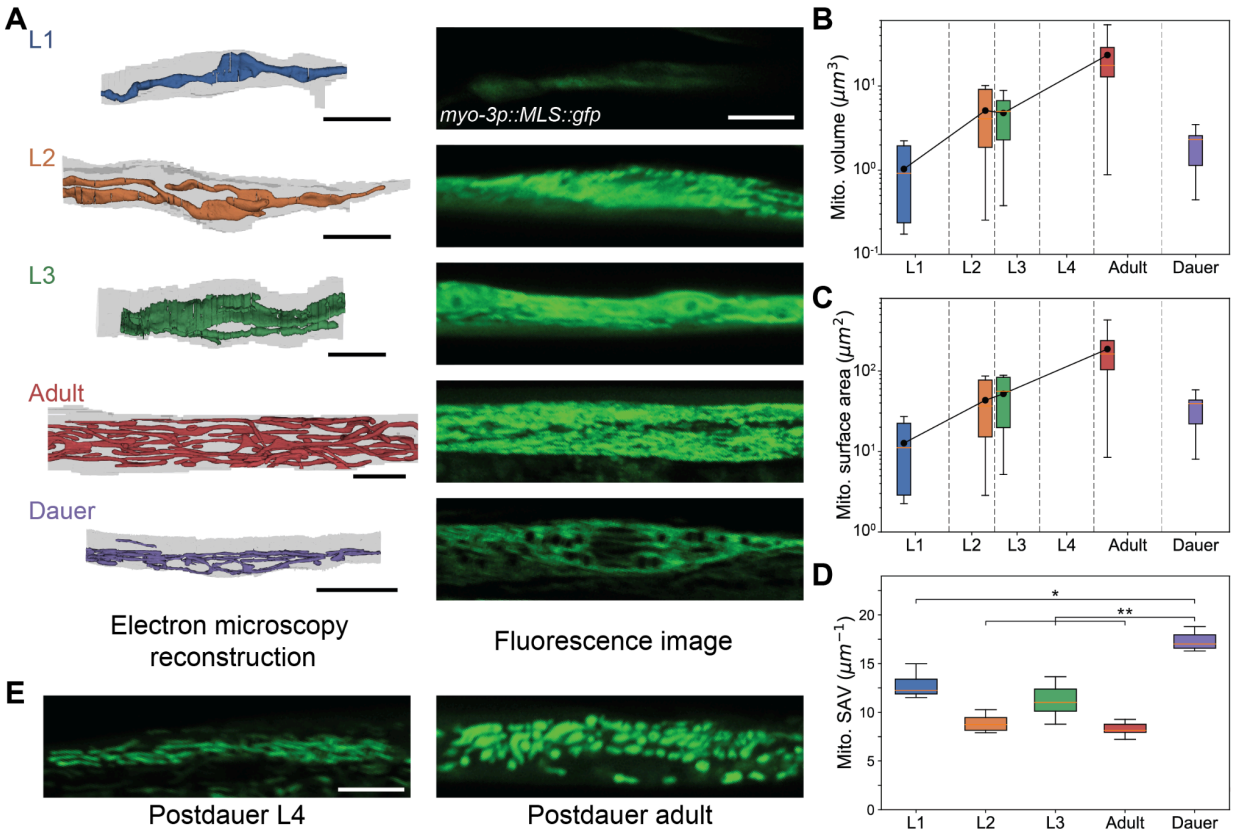

Figure 7. Mitochondria in dauer body wall muscles exhibit unique reticulum structure. (A) Reconstructed mitochondria in example body wall muscles (BWMs) in different developmental stages (left) and corresponding fluorescences images of mitochondria in BWM (right). (B) Distributions of mitochondria volume in a muscle across development. (C) Distribution of mitochondria surface area in a muscle across development. (D) Distribution of surface area per volume in a muscle in different stages. Mitochondria in dauer exhibit significantly higher surface area per volume relative to normal developmental stages (Center line: median, box: interquartile range, whiskers: 5th and 95th percentile; $*p<10^{-6}$, $**p<10^{-7}$; Wilcoxon rank-sum test). (E) Fluorescence images of BWM mitochondria in postdauer L4 (top) and postdauer adult (bottom).
(A and E) Scale bars: 5 μm (black), 5 μm (white).

strand of mitochondria, and as it matures, it branches into additional mitochondria strands (Figure 7A). Once the worm becomes an adult, the mitochondria forms a reticulum-like structure with many strands intermingled (Figure 7A). Similar developmental changes have been seen using fluorescence imaging in BWMs (Schultz et al. 2017; Han et al. 2012). In dauer, the BWMs exhibit a distinctive reticulum-like structure, which distinguishes from the adult stage, where the strands are slimmer and contain greater empty spaces, occupied by lipid droplets (Figures 7A and S7A).

To confirm that our findings are not limited to specific animals, we acquired fluorescence images of mitochondria in head and neck muscles. As shown in Figure 7A, we have verified that our observation is valid in different animals, further highlighting the distinctive reticulum-like structure in the dauer stage (Figure 7A).

Since we have high-resolution reconstruction, we can also quantify the BWM mitochondrial morphology. Consequently, we found an exponential increase in the amount of mitochondria in the cell from L1 to adulthood (Figure 7B). Dauer BWMs had less mitochondria compared to L2 and L3 as dauer BWMs include enlarged sarcomeres and space occupied by lipid droplets unlike the muscle cells in the normal reproductive stages (Figure S7A). Similar trend was observed for the surface area of the mitochondria (Figure 7C). Surface area of dauer BWM mitochondria were comparable to that of L2 and L3, resulting in significantly high surface area per volume for mitochondria in dauer BWMs (Figure 7D). This result reflects the qualitative observation that dauer BWM mitochondria is composed of thin strands (Figure 7A).

Next, we checked whether this dauer-specific mitochondria structure is preserved even after the dauer exit. Captured with fluorescence imaging, BWM mitochondria in postdauer L4 or postdauer adult stages did not show distinctive reticulum-like structure as seen in dauer (Figure 7E). Mitochondria in postdauer L4 and postdauer adult did not have empty spaces in between the strands which were filled with lipid droplets (Figure S7A).

Discussion

In this study, we present comprehensive dense reconstructions of mitochondria in normal reproductive stages and the dauer stage of *C. elegans* using 3D electron microscopy. Utilizing these reconstructed datasets, we conducted a comparative analysis of mitochondrial structures throughout development, spanning from birth to adulthood, in both neurons and body wall muscles. Consequently, we were able to propose fundamental mitochondrial structural principles shared across different stages as well as stage-specific mitochondrial structures. EM offers a distinct advantage due to its superior resolution, enabling detailed quantitative morphological comparisons that are often not feasible with fluorescence imaging, especially in small animal models such as *C. elegans*. Furthermore, our investigation encompassed the examination of mitochondria throughout the entire nervous system from sensory neurons to muscles. This provides insights into how mitochondrial structure might impact neural circuit function leading to behavioral output. Lastly, we observed unique mitochondrial structures in the alternative stage, which nematodes enter under adverse environmental conditions, suggesting potential adaptation of intracellular organelles.

Fundamental structural principles are preserved across development

We observed many structural properties of mitochondria are preserved throughout the development, including during the alternative dauer stage. The relationship between the quantity and proximity of mitochondria and the connectivity adheres to consistent rules across all stages (Figure 2). Similarly, compartment-specific mitochondrial morphology is conserved across developmental stages (Figure 3). In addition, mitochondria exhibit comparable characteristics in each cell type during normal reproductive stages (Figure 5), even when cells are classified based on the neurotransmitters they release (Figure 6). Cells and neural circuits have essential functions necessary for basic operational capabilities. Therefore, mitochondria need to follow established principles to support these essential functions.

These principles have been similarly identified in mammalian neurons. Previous studies have found the spatial distribution of synapses and mitochondria along the neurite covary, meaning synapses have mitochondria nearby potentially as an energy source and calcium buffer (Smith et al. 2016; Turner et al. 2022). Other studies have found that mitochondria in different compartments (i.e. axon, dendrites, soma) have different morphological characteristics. It has been discovered that dendritic mitochondria tend to be longer and larger than axonal mitochondria (Diane T. W. Chang, Honick, and Reynolds 2006; Lewis et al. 2018a; Turner et al. 2022). We have reported similar findings in *C. elegans* indicating the same structural principle applies even in invertebrates, further supported by a recent comprehensive study of mitochondria in *Drosophila* (Rivlin et al. 2024). This provides a link between higher order animals and *C. elegans* suggesting *C. elegans* could be a great model organism to study how mitochondria structure affects the synaptic function.

Increased mitochondria in the dauer motor neurons for dauer-specific behavior

The neurons that stand out with higher mitochondria volume fraction in dauer are interneurons (RIA, RIB; Figure 5F) and motor neurons (RMD, SMD; Figure 5F) that are known to be involved in head and neck neuromuscular system. Based on the previous observations, the dauer-specific behavior, nictation, is initiated from the head movement (Cassada and Russell 1975; H. Lee et al. 2011). The sensory neuron which regulates nictation, IL2, has been found (H. Lee et al. 2011), but the rest of the neurons in the neural circuit that generate nictation behavior are still greatly unknown despite recent efforts in dauer connectome (Yim et al. 2024).

RMD, SMD, and IL2 neurons are all cholinergic, and given acetylcholine's crucial role in neuromuscular function, it is expected to play an important role during the dauer stage (Figure 6A). Glutamatergic neurons, including RIB, are known to modulate behaviors in dauer (Zou et al. 2018). The finding that both cholinergic and glutamatergic neurons exhibit a high mitochondria volume fraction could be reflecting their important roles in the dauer stage (Figure 6F). Therefore, the neurons with higher mitochondria volume fraction in dauer could be probable candidates that regulate dauer-specific behavior, which can be tested with an optogenetics experiment (Yim et al. 2024).

Synaptic transmission not only influences the behavior but also affects developmental decision making. Previous study reported that pheromone activates ASK and ADL neurons, which in turn stimulates AIA neurons via glutamatergic transmission to induce dauer entry (Chai et al. 2022). ASK neurons have high mitochondria volume fraction in dauer as other glutamatergic neurons (Figure 6F). Also, AIA neurons are interneurons that show high mitochondria volume fraction in dauer (Figures 5D and 5F), suggesting the potential adaptation in mitochondrial structure in the dauer stage.

Mitochondria and lipid droplets in the dauer muscle cells

Previous studies using 2D cross-section analysis have shown that dauer muscle mitochondria are present in a compact conformation (Popham and Webster 1979). It is presumed that this structural property is necessary to provide large amounts of energy on a short-term basis to support rapid response behavior (Cassada and Russell 1975). This study has not only

confirmed this discovery but also extended it by uncovering the 3D structural morphology, sparse network-like structure with thin strands (Figure 7A).

Then the question naturally arises, what is present within the gaps amidst the strands? It has been reported that dauer muscle cells contain lipids unlike other developmental stages (Popham and Webster 1979). Indeed, the empty spaces between the mitochondria strands were occupied with lipid droplets (Figure S7) forming intimate contacts with mitochondria.

During the dauer stage, *C. elegans* transitions from glycolysis to using the glyoxylate cycle within mitochondria for energy production, enabling the conversion of stored fats into glucose (Burnell et al. 2005). The unique reticulum-like structure of BWM mitochondria observed in dauer (Figures 7A and 7C) may facilitate this metabolic shift. This could be a strategy adopted to increase the contact area between mitochondria and lipids to accommodate the efficient energy supply for the rapid and powerful response in dauer (Cassada and Russell 1975; O'Riordan and Burnell 1990). This result is consistent with previous findings in human skeletal muscles which showed the amount of lipid droplet and the contact area between lipids and mitochondria increased after intense exercise (Tarnopolsky et al. 2007).

Generalizable mitochondria reconstruction pipeline

We developed an automated method for detecting mitochondria in EM, allowing us to acquire dense mitochondria reconstructions across various developmental stages. Initially, we trained our detection model with the dauer EM data and subsequently enhanced the model with additional ground truth from each dataset (STAR Methods). Still, the initial model showed decent performance without fine-tuning, as mitochondria look similar in different EM datasets. Our final model, trained with all five datasets used in this study, demonstrates robust generalizability across new *C. elegans* EM datasets and potentially those from other animal models. Moreover, our model operates in 2D, making it accessible for researchers who work with single-section images to apply our method. This method could be extended to quantitatively analyze mitochondrial morphology in disease models like Huntington's disease or Alzheimer's disease, where mitochondrial dysfunction is prominent (Swerdlow 2011; Lopez Sanchez, van Wijngaarden, and Trounce 2019; Zhang et al. 2016; A. Lee et al. 2018; Liu et al. 2022; Neueder et al. 2024). All codes and models are publicly available at the GitHub repository (STAR Methods).

Acknowledgments

We thank Seok-Kyu Kwon and Yusuke Hirabayashi for valuable feedback and suggestions. Also, we would like to thank Mei Zhen's group for useful discussion and providing necessary resources. We are grateful to WormAtlas for providing invaluable resources and reference illustrations. The work was supported by the Samsung Science and Technology Foundation (SSTF-BA1501-52). J.A.B. acknowledges support by the National Research Foundation of Korea (NRF) grant (2019R1A6A1A10073437) funded by the Korean Ministry of Education. K.C.N. and D.H.H. were funded by NIH OD010943.

Author Contributions

K.C.N and D.H.H. acquired dauer EM image stack. S.B. stitched and aligned the dauer EM images. G.K., H.Y., and D.T. refined the cell segmentation of dauer dataset based on the initial segmentation generated by H.K. J.A.B. trained the mitochondria detection models and reconstructed mitochondria using the ground truth annotated by G.K. J.A.B. performed computational analysis. M.C. designed and implemented the microdroplet swimming assay and performed behavior experiments. S.A. acquired fluorescence images of body wall muscle mitochondria. S.A., M.C., D.T. acquired fluorescence images of neural mitochondria. J.A.B. wrote the paper with contributions from M.C., D.H.H., J.S.K., and J.L. J.A.B., D.H.H., J.S.K. and J.L. managed the multi-institution collaboration.

Declaration of Interests

The authors declare no competing interests.

Inclusion and Diversity

We support inclusive, diverse, and equitable conduct of research.

Methods

Electron microscopy images

For normal reproductive stages, we used electron microscopy (EM) images published by Witviet et al. (Witvliet et al. 2021) (L1: Dataset 2, L2: Dataset 5, L3: Dataset 6, Adult: Dataset 8). The raw images were acquired from Brain Observatory Storage Service and Database (BossDB) using *intern* library (Hider et al. 2022; Matelsky et al. 2021). For dauer stage, same EM dataset from Yim et al. (Yim et al. 2024) was used. Please refer to Yim et al. (Yim et al. 2024) for details.

Volumetric cell segmentation

For normal reproductive stages, we used volumetrically segmented cell reconstructions published by (Witvliet et al. 2021) (L1: Dataset 2, L2: Dataset 5, L3: Dataset 6, Adult: Dataset 8). The segmentation images were acquired from BossDB using *intern* library (Hider et al. 2022; Matelsky et al. 2021). For body wall muscle segmentation, an annotator painted body wall muscles in every 8th section. Then, the intermediate sections were filled by the painted result of the closest section.

Volumetric cell segmentation for dauer images were manually segmented by painting individual sections using VAST (Berger, Seung, and Lichtman 2018). Unlike normal reproductive stages, body wall muscles were painted in every section like other cells in the volume.

Synapses and connectivity graph

For normal reproductive stages, we used synapses and connectivity information published by Witvliet et al. (Witvliet et al. 2021), publicly available at BossDB (Hider et al. 2022).

Ground truth annotation for mitochondria detection

For normal reproductive stages and the dauer stage EM image stacks, we picked 10 to 20 sections from each stage. All mitochondria in each section were manually labeled using VAST (Berger, Seung, and Lichtman 2018) and saved as binary images. For dauer stage, synapses and connectivity information generated in Yim et al. (Yim et al. 2024).

Cell type classification

Cell types based on neuronal function (sensory, inter-, motor neurons) were defined according to classification defined in WormAtlas. If there are multiple types per neuron, we defined it as its primary role. The cell types we have used is consistent with what we have used in Yim et al. (Yim et al. 2024).

Cell types based on the neurotransmitter types (acetylcholine, glutamate, dopamine, GABA, octopamine) were defined according to classification defined in Hobert et al. (Hobert, Glenwinkel, and White 2016). Only primary neurotransmitters were used for classification.

Mitochondria reconstruction

In every EM image section, mitochondria were detected using deep learning. The network used for the mitochondria detection was adopted from 2D symmetric U-Net architecture (Ronneberger, Fischer, and Brox 2015). The architecture was composed of five layers with a number of feature maps 16, 32, 64, 128, 256 from the top most layer to the bottom most layer, respectively. For each step in downsampling and upsampling layers, the architecture consisted of three 3 x 3 non-strided same convolutions. In the downsampling layers, max pooling was used to downsample by a factor of 2 in each layer. In the upsampling layers, a transposed convolution layer with nearest neighbor interpolation followed by 2 x 2 non-strided convolution was used to upsample by a factor of 2 in each layer. Skip connection was included in every layer which concatenates feature maps at the same level of the left hand side to the output of the transposed convolution layer. Instance normalization (Ulyanov, Vedaldi, and Lempitsky 2016) and rectified linear unit (ReLU) was added after each 3 x 3 convolution. At the end of the symmetric network, 3 x 3 non-strided same convolution and sigmoid function was applied to produce the same-sized output image, where each pixel value represents probability of each pixel belonging to mitochondria.

From the probability map, we thresholded the image with a pixel threshold of 128 / 255 (50%) and generated binarized prediction images of mitochondria. To reconstruct 3D mitochondria, we applied connected components with connectivity of 26. The errors in resulting reconstructions were corrected manually.

All the mitochondria were skeletonized using Kimimaro (Silversmith et al. 2022, 2021).

Computation of synaptic properties

Out- and in-degrees were calculated by counting the total number of postsynaptic and presynaptic partners respectively. For example, if there's 3 postsynaptic partners for an active

zone, 3 will be added to compute out-degree. Synapse size is approximated by measuring the size of the active zone. We count the number of voxels, then multiply by the voxel resolution to get the physical size of an active zone. In this paper, the terms “active zone size” and “synapse size” are used interchangeably. Fan-out is a measure that is computed for each active zone, indicating the number of postsynaptic partners per active zone. Cells with either 0 out- or in-degree are neglected from the corresponding analyses.

Computation of mitochondrial properties

Number of mitochondria is the total number of mitochondria in a cell. Mitochondria volume indicates the size of each mitochondria. The volume is calculated by multiplying the voxel count by the voxel resolution. For analyses done per cell, mitochondria volume means total sum of volumes of all mitochondria included in a cell (Figures 5-7). Mitochondria volume fraction is an proxy for mitochondrial density of each cell. The volume fraction is computed by dividing the total mitochondria volume in a cell by the volume of a cell. Mitochondria surface area per volume (SAV) is calculated by dividing the total sum of surface area of all mitochondria by the total sum of volumes of all mitochondria. Mitochondria complexity index (MCI) (Vincent et al. 2019) was computed as

$$MCI = \frac{SA^3}{16\pi^2 V^2}$$

where SA is the surface area and V is the volume of mitochondria. Cells without any mitochondria have been neglected from the corresponding analyses.

Computation of distance between synapses and mitochondria

Mitochondria positions were determined by the centroids of segmented mitochondria and the positions of presynaptic sites were determined by the centroids of segmented active zones. For postsynaptic sites, the positions were assigned to the active zone positions for corresponding presynaptic partners. Depending on the analysis, we either measured distance to nearest mitochondria from pre- (d_{mito}^{pre}) and postsynaptic (d_{mito}^{post}) sites, or distance from each mitochondria to nearest pre- (d_{syn}^{pre}) and postsynaptic (d_{syn}^{pre}) sites by calculating the euclidean distance between two positions.

For randomizations used in Figures 2C and 2D, we assigned random mitochondria within the same neuron instead of the nearest mitochondria for each active zone and measured the distance. 1000 random configurations have been generated and mean and 95% confidence intervals are shown in Figure 2C. In Figure 2D, distribution of distances from one randomly selected configuration is shown as representative.

Microdroplet swimming assay

A microdroplet swimming assay was performed to simultaneously measure the frequency of reorientation in a large number of nematodes. Young adult animals were grown on standard nematode growth medium plates containing E. coli OP50. Nematodes in the food lawn were

washed in M9 solution to remove *E. coli* attached to their bodies, and their behavior was measured by placing them in 1.5 microliters of M9. Swimming and reorientation behavior videos were recorded at 10 Hz. Custom algorithm was used to measure turning rates in micro-droplets (Choi et al. 2020).

Principal component analysis of mitochondrial features

To investigate the overview of mitochondrial features, five structural features of mitochondria in a neuron were used: Mean mitochondria volume, mean mitochondria surface area, mean mitochondria length, mitochondria volume fraction, and mean mitochondria complexity index. The features were standardized and projected onto the first two principal components.

Sample preparation and fluorescence imaging

Confocal microscopy (ZEISS LSM700; Carl Zeiss) was used to observe mitochondrial transgene expression in the body wall muscle of *C. elegans*. For microscopy and imaging, transgenic animals were paralyzed with 3 mM levamisole and mounted on 3% agar pads. All transgenic animals were observed and imaged at the stage as described: L1, L2, L3, L4, Day 0 adult, Day 5 adult, dauer, Day 0 postdauer adult, Day 5 postdauer adult. All stage worms were collected after *C. elegans* synchronization (L1) with cultivation during proper developmental time except dauer and postdauer adult.

Neurons and mitochondria renderings

All the renderings of neurons and mitochondria were created in Python using MeshParty (github.com/CAVEconnectome/MeshParty). Screenshots of Neuroglancer (https://github.com/google/neuroglancer) were used for some figures (Figure S5).

Statistical testing

To find the significance in linear correlation, Pearson correlation was used (Figures 2 and S2). For comparing two independent distributions, Wilcoxon rank-sum test was used as most of the distributions did not follow the normal distribution (Figures 2-7 and S2). Significance tests with p values less than 10^{-20} were marked as $p \approx 0$.

Data and code availability

Mitochondria reconstruction and analysis code is available at https://github.com/jabae/Cmito. EM images, cell segmentation images, and connectivity data (Witvliet et al. 2021; Yim et al. 2024) are available in BossDB. Mitochondria reconstructions of all development stages are available upon request.

References

Altun, Z.F. and Hall, D.H. 2024. “Handbook of C. Elegans Anatomy.” *WormAtlas*.

Berger, Daniel R., H. Sebastian Seung, and Jeff W. Lichtman. 2018. “VAST (Volume Annotation and Segmentation Tool): Efficient Manual and Semi-Automatic Labeling of Large 3D Image Stacks.” *Frontiers in Neural Circuits* 12 (October): 88.

Bloss, Erik B., Mark S. Cembrowski, Bill Karsh, Jennifer Colonell, Richard D. Fetter, and Nelson Spruston. 2018. “Single Excitatory Axons Form Clustered Synapses onto CA1 Pyramidal Cell Dendrites.” *Nature Neuroscience* 21 (3): 353–63.

Burnell, Ann M., Koen Houthoofd, Karen O’Hanlon, and Jacques R. Vanfleteren. 2005. “Alternate Metabolism during the Dauer Stage of the Nematode Caenorhabditis Elegans.” *Experimental Gerontology* 40 (11): 850–56.

Calì, Corrado, Marta Wawrzyniak, Carlos Becker, Bohumil Maco, Marco Cantoni, Anne Jorstad, Biagio Nigro, et al. 2018. “The Effects of Aging on Neuropil Structure in Mouse Somatosensory cortex—A 3D Electron Microscopy Analysis of Layer 1.” *PloS One* 13 (7): e0198131.

Cassada, R. C., and R. L. Russell. 1975. “The Dauerlarva, a Post-Embryonic Developmental Variant of the Nematode Caenorhabditis Elegans.” *Developmental Biology* 46 (2): 326–42.

Chai, Cynthia M., Mahdi Torkashvand, Maedeh Seyedolmohadesin, Heenam Park, Vivek Venkatachalam, and Paul W. Sternberg. 2022. “Interneuron Control of C. Elegans Developmental Decision-Making.” *Current Biology: CB* 32 (10): 2316–24.e4.

Chang, Diane T. W., Anthony S. Honick, and Ian J. Reynolds. 2006. “Mitochondrial Trafficking to Synapses in Cultured Primary Cortical Neurons.” *The Journal of Neuroscience: The Official Journal of the Society for Neuroscience* 26 (26): 7035–45.

Chang, D. T. W., A. S. Honick, and I. J. Reynolds. 2006. “Mitochondrial Trafficking to Synapses in Cultured Primary Cortical Neurons.” *Journal of Neuroscience* 26 (26): 7035–45.

Choi, Myung-Kyu, He Liu, Taihong Wu, Wenxing Yang, and Yun Zhang. 2020. “NMDAR-Mediated Modulation of Gap Junction Circuit Regulates Olfactory Learning in C. Elegans.” *Nature Communications* 11 (1): 3467.

Courchet, Julien, Tommy L. Lewis Jr, Sohyon Lee, Virginie Courchet, Deng-Yuan Liou, Shinichi Aizawa, and Franck Polleux. 2013. “Terminal Axon Branching Is Regulated by the LKB1-NUAK1 Kinase Pathway via Presynaptic Mitochondrial Capture.” *Cell* 153 (7): 1510–25.

Gaglia, Marta Maria, and Cynthia Kenyon. 2009. “Stimulation of Movement in a Quiescent, Hibernation-like Form of Caenorhabditis Elegans by Dopamine Signaling.” *The Journal of Neuroscience: The Official Journal of the Society for Neuroscience* 29 (22): 7302–14.

Golden, J. W., and D. L. Riddle. 1984a. “A Pheromone-Induced Developmental Switch in Caenorhabditis Elegans: Temperature-Sensitive Mutants Reveal a Wild-Type Temperature-Dependent Process.” *Proceedings of the National Academy of Sciences of the United States of America* 81 (3): 819–23.

———. 1984b. “The Caenorhabditis Elegans Dauer Larva: Developmental Effects of Pheromone, Food, and Temperature.” *Developmental Biology* 102 (2): 368–78.

Gray, Jesse M., Joseph J. Hill, and Cornelia I. Bargmann. 2005. “A Circuit for Navigation in Caenorhabditis Elegans.” *Proceedings of the National Academy of Sciences of the United States of America* 102 (9): 3184–91.

Grueber, Wesley B., Chung-Hui Yang, Bing Ye, and Yuh-Nung Jan. 2005. “The Development of Neuronal Morphology in Insects.” *Current Biology: CB* 15 (17): R730–38.

Hallem, Elissa A., Adler R. Dillman, Annie V. Hong, Yuanjun Zhang, Jessica M. Yano, Stephanie F. DeMarco, and Paul W. Sternberg. 2011. “A Sensory Code for Host Seeking in Parasitic Nematodes.” *Current Biology: CB* 21 (5): 377–83.

Han, Sung Min, Hiroshi Tsuda, Youfeng Yang, Jack Vibbert, Pauline Cottee, Se-Jin Lee, Jessica Winek, Claire Haueter, Hugo J. Bellen, and Michael A. Miller. 2012. “Secreted VAPB/ALS8 Major Sperm Protein Domains Modulate Mitochondrial Localization and Morphology via Growth Cone Guidance Receptors.” *Developmental Cell* 22 (2): 348–62.

Harris, Julia J., Renaud Jolivet, and David Attwell. 2012. “Synaptic Energy Use and Supply.” *Neuron* 75 (5): 762–77.

Hendricks, Michael, Heonick Ha, Nicolas Maffey, and Yun Zhang. 2012. “Compartmentalized

Calcium Dynamics in a C. Elegans Interneuron Encode Head Movement." *Nature* 487 (7405): 99–103.
Hider, Robert, Jr, Dean Kleissas, Timothy Gion, Daniel Xenes, Jordan Matelsky, Derek Pryor, Luis Rodriguez, Erik C. Johnson, William Gray-Roncal, and Brock Wester. 2022. "The Brain Observatory Storage Service and Database (BossDB): A Cloud-Native Approach for Petascale Neuroscience Discovery." *Frontiers in Neuroinformatics* 16 (February): 828787.
Hobert, Oliver, Lori Glenwinkel, and John White. 2016. "Revisiting Neuronal Cell Type Classification in Caenorhabditis Elegans." *Current Biology: CB* 26 (22): R1197–1203.
Kann, Oliver. 2016. "The Interneuron Energy Hypothesis: Implications for Brain Disease." *Neurobiology of Disease* 90 (June): 75–85.
Kasthuri, Narayanan, Kenneth Jeffrey Hayworth, Daniel Raimund Berger, Richard Lee Schalek, José Angel Conchello, Seymour Knowles-Barley, Dongil Lee, et al. 2015. "Saturated Reconstruction of a Volume of Neocortex." *Cell* 162 (3): 648–61.
Khalil, Reem, Ahmad Farhat, and Paweł Dłotko. 2021. "Developmental Changes in Pyramidal Cell Morphology in Multiple Visual Cortical Areas Using Cluster Analysis." *Frontiers in Computational Neuroscience* 15 (May): 667696.
Kimura, Toshiya, and Fujio Murakami. 2014. "Evidence That Dendritic Mitochondria Negatively Regulate Dendritic Branching in Pyramidal Neurons in the Neocortex." *The Journal of Neuroscience: The Official Journal of the Society for Neuroscience* 34 (20): 6938–51.
Kolk, Sharon M., and Pasko Rakic. 2022. "Development of Prefrontal Cortex." *Neuropsychopharmacology: Official Publication of the American College of Neuropsychopharmacology* 47 (1): 41–57.
Kroon, Tim, Eline van Hugte, Lola van Linge, Huibert D. Mansvelder, and Rhiannon M. Meredith. 2019. "Early Postnatal Development of Pyramidal Neurons across Layers of the Mouse Medial Prefrontal Cortex." *Scientific Reports* 9 (1): 5037.
Lee, Annie, Yusuke Hirabayashi, Seok-Kyu Kwon, Tommy L. Lewis Jr, and Franck Polleux. 2018. "Emerging Roles of Mitochondria in Synaptic Transmission and Neurodegeneration." *Current Opinion in Physiology* 3 (June): 82–93.
Lee, Harksun, Myung-Kyu Choi, Daehan Lee, Hye-Sung Kim, Hyejin Hwang, Heekyeong Kim, Sungsu Park, Young-Ki Paik, and Junho Lee. 2011. "Nictation, a Dispersal Behavior of the Nematode Caenorhabditis Elegans, Is Regulated by IL2 Neurons." *Nature Neuroscience* 15 (1): 107–12.
Lewis, Tommy L., Jr, Seok-Kyu Kwon, Annie Lee, Reuben Shaw, and Franck Polleux. 2018a. "MFF-Dependent Mitochondrial Fission Regulates Presynaptic Release and Axon Branching by Limiting Axonal Mitochondria Size." *Nature Communications* 9 (1): 5008.
Lewis, Tommy L., Seok-Kyu Kwon, Annie Lee, Reuben Shaw, and Franck Polleux. 2018b. "MFF-Dependent Mitochondrial Fission Regulates Presynaptic Release and Axon Branching by Limiting Axonal Mitochondria Size." *Nat. Communications*, November. https://doi.org/10.1101/276691.
Liu, Chunyue, Zixing Fu, Shanshan Wu, Xiaosong Wang, Shengrong Zhang, Chu Chu, Yuan Hong, et al. 2022. "Mitochondrial HSF1 Triggers Mitochondrial Dysfunction and Neurodegeneration in Huntington's Disease." *EMBO Molecular Medicine* 14 (7): e15851.
Lopez Sanchez, M. Isabel G., Peter van Wijngaarden, and Ian A. Trounce. 2019. "Amyloid Precursor Protein-Mediated Mitochondrial Regulation and Alzheimer's Disease." *British Journal of Pharmacology* 176 (18): 3464–74.
Matelsky, Jordan K., Luis M. Rodriguez, Daniel Xenes, Timothy Gion, Robert Hider, Brock A. Wester, and William Gray-Roncal. 2021. "An Integrated Toolkit for Extensible and Reproducible Neuroscience." *Conference Proceedings: ... Annual International Conference of the IEEE Engineering in Medicine and Biology Society. IEEE Engineering in Medicine and Biology Society. Conference* 2021 (November): 2413–18.
Mulcahy, Ben, Daniel K. Witvliet, James Mitchell, Richard Schalek, Daniel R. Berger, Yuelong

Wu, Doug Holmyard, et al. 2022. “Post-Embryonic Remodeling of the C. Elegans Motor Circuit.” *Current Biology: CB* 32 (21): 4645–59.e3.
Neueder, Andreas, Kerstin Kojer, Zhenglong Gu, Yiqin Wang, Tanja Hering, Sarah Tabrizi, Jan-Willem Taanman, and Michael Orth. 2024. “Huntington’s Disease Affects Mitochondrial Network Dynamics Predisposing to Pathogenic Mitochondrial DNA Mutations.” *Brain: A Journal of Neurology* 147 (6): 2009–22.
Neural Circuit Development and Function in the Healthy and Diseased Brain: Comprehensive Developmental Neuroscience. 2013. Academic Press.
O’Riordan, Veronica B., and Ann M. Burnell. 1990. “Intermediary Metabolism in the Dauer Larva of the Nematode Caenorhabditis elegans—II. The Glyoxylate Cycle and Fatty-Acid Oxidation.” *Comparative Biochemistry and Physiology Part B: Comparative Biochemistry* 95 (1): 125–30.
Pierce-Shimomura, J. T., T. M. Morse, and S. R. Lockery. 1999. “The Fundamental Role of Pirouettes in Caenorhabditis Elegans Chemotaxis.” *The Journal of Neuroscience: The Official Journal of the Society for Neuroscience* 19 (21): 9557–69.
Popham, J. D., and J. M. Webster. 1979. “Aspects of the Fine Structure of the Dauer Larva of the Nematode Caenorhabditis Elegans.” *Canadian Journal of Zoology* 57 (4): 794–800.
Riboul, Danielle V., Sarah Crill, Carlos Oliva, Maria Gabriela Restifo, Reggie Joseph, Kerdes Joseph, Ken C. Q. Nguyen, David H. Hall, Yaouen Fily, and Gregory T. Macleod. 2023. “Ultrastructural Analysis Reveals Mitochondrial Placement Independent of Synapse Placement in Fine Caliber C. Elegans Neurons.” *bioRxiv : The Preprint Server for Biology*, June. https://doi.org/10.1101/2023.05.30.542959.
Rivlin, Patricia K., Michal Januszewski, Kit D. Longden, Erika Neace, Louis K. Scheffer, Christopher Ordish, Jody Clements, et al. 2024. “Connectomic Analysis of Mitochondria in the Central Brain of Drosophila.” *bioRxiv*. https://doi.org/10.1101/2024.04.21.590464.
Ronneberger, Olaf, Philipp Fischer, and Thomas Brox. 2015. “U-Net: Convolutional Networks for Biomedical Image Segmentation.” In *Medical Image Computing and Computer-Assisted Intervention – MICCAI 2015*, 234–41. Springer International Publishing.
Schultz, Jessica, Se-Jin Lee, Tim Cole, Hieu D. Hoang, Jack Vibbert, Pauline A. Cottee, Michael A. Miller, and Sung Min Han. 2017. “The Secreted MSP Domain of C. Elegans VAPB Homolog VPR-1 Patterns the Adult Striated Muscle Mitochondrial Reticulum via SMN-1.” *Development* 144 (12): 2175–86.
Sheng, Zu-Hang, and Qian Cai. 2012. “Mitochondrial Transport in Neurons: Impact on Synaptic Homeostasis and Neurodegeneration.” *Nature Reviews. Neuroscience* 13 (2): 77–93.
Silversmith, William, J. Alexander Bae, Peter H. Li, and A. M. Wilson. 2021. *Kimimaro: Skeletonize Densely Labeled 3D Image Segmentations* (version 3.0.0). https://doi.org/10.5281/zenodo.5539913.
Silversmith, William, Aleksandar Zlateski, J. Alexander Bae, Ignacio Tartavull, Nico Kemnitz, Jingpeng Wu, and H. Sebastian Seung. 2022. “Igneous: Distributed Dense 3D Segmentation Meshing, Neuron Skeletonization, and Hierarchical Downsampling.” *Frontiers in Neural Circuits* 16 (November): 977700.
Smith, Heather L., Jennifer N. Bourne, Guan Cao, Michael A. Chirillo, Linnaea E. Ostroff, Deborah J. Watson, and Kristen M. Harris. 2016. “Mitochondrial Support of Persistent Presynaptic Vesicle Mobilization with Age-Dependent Synaptic Growth after LTP.” *eLife* 5 (December). https://doi.org/10.7554/eLife.15275.
Swerdlow, Russell H. 2011. “Brain Aging, Alzheimer’s Disease, and Mitochondria.” *Biochimica et Biophysica Acta* 1812 (12): 1630–39.
Tarnopolsky, Mark A., Courtney D. Rennie, Holly A. Robertshaw, Stephanie N. Fedak-Tarnopolsky, Michaela C. Devries, and Mazen J. Hamadeh. 2007. “Influence of Endurance Exercise Training and Sex on Intramyocellular Lipid and Mitochondrial Ultrastructure, Substrate Use, and Mitochondrial Enzyme Activity.” *American Journal of*

Physiology. Regulatory, Integrative and Comparative Physiology 292 (3): R1271–78.
Tau, Gregory Z., and Bradley S. Peterson. 2010. “Normal Development of Brain Circuits.” *Neuropsychopharmacology: Official Publication of the American College of Neuropsychopharmacology* 35 (1): 147–68.
Turner, Nicholas L., Thomas Macrina, J. Alexander Bae, Runzhe Yang, Alyssa M. Wilson, Casey Schneider-Mizell, Kisuk Lee, et al. 2022. “Reconstruction of Neocortex: Organelles, Compartments, Cells, Circuits, and Activity.” *Cell* 185 (6): 1082–1100.e24.
Ulyanov, Dmitry, Andrea Vedaldi, and Victor Lempitsky. 2016. “Instance Normalization: The Missing Ingredient for Fast Stylization.” *arXiv [cs.CV]*. arXiv. http://arxiv.org/abs/1607.08022.
Verstreken, Patrik, Cindy V. Ly, Koen J. T. Venken, Tong-Wey Koh, Yi Zhou, and Hugo J. Bellen. 2005. “Synaptic Mitochondria Are Critical for Mobilization of Reserve Pool Vesicles at Drosophila Neuromuscular Junctions.” *Neuron* 47 (3): 365–78.
Vincent, Amy E., Kathryn White, Tracey Davey, Jonathan Philips, R. Todd Ogden, Conor Lawless, Charlotte Warren, et al. 2019. “Quantitative 3D Mapping of the Human Skeletal Muscle Mitochondrial Network.” *Cell Reports* 27 (1): 321.
White, J. G., E. Southgate, J. N. Thomson, and S. Brenner. 1986. “The Structure of the Nervous System of the Nematode *Caenorhabditis Elegans*.” *Philosophical Transactions of the Royal Society of London. Series B, Biological Sciences* 314 (1165): 1–340.
Witvliet, Daniel, Ben Mulcahy, James K. Mitchell, Yaron Meirovitch, Daniel R. Berger, Yuelong Wu, Yufang Liu, et al. 2021. “Connectomes across Development Reveal Principles of Brain Maturation.” *Nature* 596 (7871): 257–61.
Wolkow, C. A., and D. H. Hall. 2016. “Handbook of C. Elegans Dauer Anatomy.” *WormAtlas*. http://www.wormatlas.org/dauer/dauerhomepage.htm.
Yim, Hyunsoo, Daniel T. Choe, J. Alexander Bae, Myung-Kyu Choi, Hae-Mook Kang, Ken C. Q. Nguyen, Soungyub Ahn, et al. 2024. “Comparative Connectomics of Dauer Reveals Developmental Plasticity.” *Nature Communications* 15 (1): 1546.
Zhang, Liang, Sergey Trushin, Trace A. Christensen, Benjamin V. Bachmeier, Benjamin Gateno, Andreas Schroeder, Jia Yao, et al. 2016. “Altered Brain Energetics Induces Mitochondrial Fission Arrest in Alzheimer’s Disease.” *Scientific Reports* 6 (January): 18725.
Zou, Wenjuan, Jiajun Fu, Haining Zhang, Kang Du, Wenming Huang, Junwei Yu, Shitian Li, et al. 2018. “Decoding the Intensity of Sensory Input by Two Glutamate Receptors in One C. Elegans Interneuron.” *Nature Communications* 9 (1): 4311.